Detection of Drug Binding to DNA by Hydroxyl Radical Footprinting. Relationship of Distamycin Binding Sites to DNA Structure and Positioned Nucleosomes on 5S RNA Genes of *Xenopus*†

Mair E. A. Churchill,‡ Jeffrey J. Hayes, and Thomas D. Tullius*
Department of Chemistry, The Johns Hopkins University, Baltimore, Maryland 21218
Received December 6, 1989; Revised Manuscript Received March 29, 1990

ABSTRACT: We report the use of hydroxyl radical footprinting to analyze the interaction of distamycin and actinomycin with the 5S ribosomal RNA genes of *Xenopus*. There is a qualitative difference in the hydroxyl radical footprints of the two drugs. Distamycin gives a conventional (albeit high-resolution) footprint, while actinomycin does not protect DNA from hydroxyl radical attack, but instead induces discrete sites of hyperreactivity. We find concentration-dependent changes in the locations of distamycin binding sites on the somatic 5S gene of *Xenopus borealis*. A high-affinity site, containing a G·C base pair, is replaced at higher levels of bound drug by a periodic array of different lower affinity sites that coincide with the places where the minor groove of the DNA would face in toward a nucleosome core that is known to bind to the same sequence. These results suggest that distamycin recognizes potential binding sites more by the shape of the DNA than by the specific sequence that is contained in the site and that structures of many sequences are deformable to a shape that allows drug binding. We discuss the utility of hydroxyl radical footprinting of distamycin for investigating the underlying structure of DNA.

Several classes of antitumor drugs and antibiotics exhibit biological efficacy as the result of direct interaction with DNA. Numerous studies (Neidle & Abraham, 1984; Zimmer & Wähnert, 1986), including footprinting experiments (Van Dyke et al., 1979; Lane et al., 1983; Fox & Waring, 1984; Kuwabara et al., 1986; Portugal & Waring, 1987; Ward et al., 1988; Cons & Fox, 1989a,b), on complexes of DNA with actinomycin, netropsin, distamycin, mithramycin, and Hoechst 33258 have shown that these drugs bind to the minor groove of DNA. Intercalating drugs such as actinomycin were found to bind to G/C-rich sequences that contain a GpC base step. The nonintercalators distamycin and netropsin have been reported to bind to A/T-rich stretches 4–5 base pairs (bp)[1] in length. The structures of complexes of oligonucleotides with netropsin, Hoechst 33258, and distamycin have been determined in solution by NMR (Patel, 1982; Patel et al., 1982; Feigon et al., 1984; Klevit et al., 1986; Pelton & Wemmer, 1988, 1989), and in the solid state using X-ray crystallography (Kopka et al., 1985a,b; Coll et al., 1987, 1989). The results of atomic resolution structural studies suggest that these drugs bind in the minor groove of DNA and replace the spine of hydration (Kopka et al., 1985a,b).

The preference of distamycin for binding to A/T-rich sequences is thought to be due to the properties of the minor groove of these sequences, which is distinctly narrow and lacking 2-amino groups that protrude from the floor of the groove. Distamycin is fully engulfed by the minor groove in A/T-rich regions, allowing many productive van der Waals and hydrogen bonding interactions (Coll et al., 1987). However, at high drug:DNA ratios, some lower affinity sites which contain G·C base pairs have been identified (Zimmer & Wähnert, 1986). How closely the structure of the distamycin–DNA complex in these low-affinity binding sites resembles the structure adopted in the high-affinity sites is not well understood.

We report here the use of the hydroxyl radical footprinting technique to study the complexes of distamycin and actinomycin with 5S ribosomal RNA genes of *Xenopus*. This method has been used to obtain high-resolution structural data on a number of different DNA molecules and DNA–protein complexes (Tullius et al., 1987; Tullius, 1987). Previously, application of hydroxyl radical footprinting to drug–DNA complexes was reported for distamycin and netropsin (Portugal & Waring, 1987), mithramycin (Cons & Fox, 1989a,b), and actinomycin and nogalamycin (Fox, 1988).

The hydroxyl radical, which we generate by the reduction of hydrogen peroxide by EDTA·Fe(II), is a small, very reactive species that abstracts a hydrogen atom from the deoxyribose, leading to DNA strand scission at the point of attack. The hydroxyl radical is a relatively non-sequence-specific cleavage agent, and so, in contrast to deoxyribonuclease I (DNase I) footprinting, information is made available on drug–DNA contacts throughout a DNA molecule. Moreover, the small size of the hydroxyl radical results in very high-resolution footprints of molecules bound to DNA.

We compare the footprints of distamycin and actinomycin obtained by methidiumpropyl-EDTA·iron(II) [MPE·Fe(II)] to protection patterns generated by hydroxyl radical cleavage, to illustrate the higher resolution (at least in the case of distamycin) available using the hydroxyl radical footprinting method (Portugal & Waring, 1987). The increased resolution allowed us to detect an unusual feature of distamycin binding to the 5S gene. We find that at low concentration of drug, distamycin first binds to a single high-affinity site in the 5S gene that contains a G·C base pair, although other sites con-

† This research was supported by USPHS Grants CA 37444 and GM 40894. T.D.T. is a fellow of the Alfred P. Sloan Foundation and is the recipient of a Research Career Development Award from the National Cancer Institute of the NIH (CA 01208) and a Camille and Henry Dreyfus Teacher–Scholar Award.
* Address correspondence to this author.
‡ Present address: MRC Laboratory of Molecular Biology, Hills Road, Cambridge CB2 2QH, U.K.

[1] Abbreviations: bp, base pair(s); DNase I, deoxyribonuclease I; EDTA, disodium ethylenediaminetetraacetic acid; MPE·Fe(II), methidiumpropyl-EDTA·iron(II); r_i, [drug added]/[DNA phosphate]; TFIIIA, transcription factor IIIA.

0006-2960/90/0429-6043$02.50/0

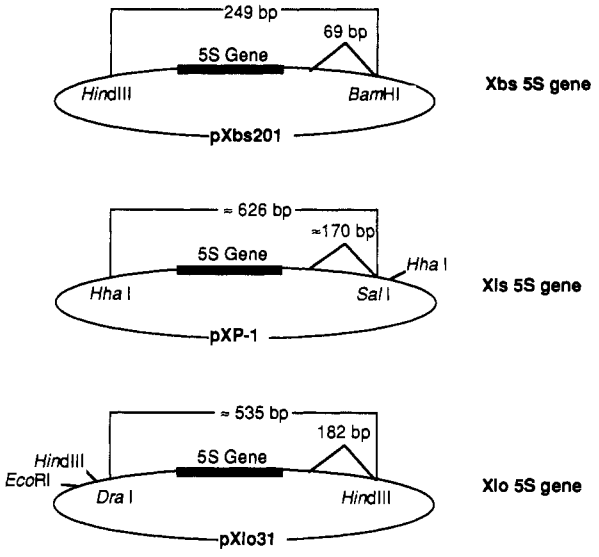

FIGURE 1: Diagrams of the plasmids used in these experiments, showing the restriction fragments containing the 5S ribosomal RNA genes of *Xenopus borealis* (Xbs) and *Xenopus laevis* (Xls, Xlo) that were used for footprinting of actinomycin and distamycin.

sisting of runs of adenines are available and unoccupied. At higher levels of bound drug, distamycin appears to vacate the high-affinity site and bind to an array of lower affinity sites. We noticed a periodic pattern in these low-affinity distamycin binding sites which corresponds to the way in which a positioned nucleosome binds to the same DNA (Rhodes, 1985; Losa & Brown, 1987).

This result highlights a second motivation for the present experiments: the possibility that groove binding drugs might be useful as probes of the structure of DNA in solution. The sensitivity of distamycin binding to small conformational differences in DNA, for example, might indicate places where the helix deviates from the classic B-type structure and exhibits an altered minor groove conformation, such as that found in the A-type helix. The 5S RNA gene is a good candidate for such a study because there is a protein, transcription factor IIIA (TFIIIA), that binds not only to positions +45 to +95 in the 5S gene DNA (called the internal control region) (Figure 1) but also to the gene product, 5S RNA. One explanation of how TFIIIA might recognize both RNA and DNA is that the DNA adopts a conformation that is somewhat RNA-like (or more like the A form).

Earlier studies showed that netropsin and distamycin do not bind to RNA, to DNA–RNA hybrids, or to A-DNA (Zimmer, 1975). Zimmer et al. (1984) showed that these drugs are capable, at high concentrations, of inducing the A- to B-DNA transition, by stabilizing the B-DNA conformation. We were inspired by these results to use hydroxyl radical footprinting to screen the 5S gene for distamycin binding sites. Sequences to which the drug does not bind at low concentration might be candidates for having a non-B-DNA conformation.

Experimental Procedures

Preparation and End-Labeling of DNA. The plasmids pXbs201 [that contains the somatic 5S ribosomal RNA gene from *Xenopus borealis* (Xbs) (Bogenhagen et al., 1980)], pXP-1 [that contains the *Xenopus laevis* somatic (Xls) 5S RNA gene (Wolffe & Brown, 1987)], and pXlo31 [that contains the *Xenopus laevis* oocyte (Xlo) 5S RNA gene (Miller at al., 1978)] (shown schematically in Figure 1) were transformed into *Escherichia coli*, isolated, and purified by using a modified version of the cleared lysate procedure for plasmid DNA isolation (Tullius et al., 1987). Plasmid pXbs201 was labeled with radioactive phosphorus by standard methods at either the 5′ or the 3′ end of the *Bam*HI- or *Hin*dIII-cut plasmid. Plasmid pXP-1 was first cleaved with *Sal*I, 3′ end-labeled, and cleaved a second time with *Hha*I, for radioactive labeling of the noncoding strand. Plasmid pXlo31 was cleaved with *Hin*dIII, 3′ end-labeled, and cleaved again by digestion with *Dra*I and *Eco*RI to label the noncoding strand. Radioactively labeled DNA restriction fragments were separated by electrophoresis on an 8% native polyacrylamide gel. Labeled DNA was recovered and purified from the gel by using a modified version of the Maxam and Gilbert (1980) crush and soak procedure, which included one phenol extraction followed by ether extraction and ethanol precipitation.

Drug Binding to DNA. Radioactively labeled DNA (approximately 70000 cpm) and 0.1 μg of carrier (sonicated calf thymus) DNA were added to a buffer consisting of 20 mM HEPES (pH 7.4), 140 mM ammonium chloride, 7 mM $MgCl_2$, and 10 μM $ZnCl_2$, in a volume of 35 μL. [This buffer is similar to the one used for TFIIIA binding (Smith et al., 1984) except that it lacks NP-40 and bovine serum albumin.] Actinomycin was added in an amount such that its final concentration (after adding the footprinting reagents, see below) would be 100 μM. Similarly, the appropriate amount of distamycin was added so that its final concentration would be 4.7 μM, or the concentrations needed for the titration experiments. Concentrations of drugs in stock solutions were determined by spectrophotometry. The DNA–drug solutions were allowed to stand at room temperature for 30 min.

Footprinting with the Hydroxyl Radical. The hydroxyl radical generating cleavage reagent was allowed to react with DNA in the presence or absence of drug for 2 min at room temperature. Cleavage was initiated by introducing 5 μL each of 100 μM iron(II), 200 μM EDTA, 0.3% H_2O_2, and 10 mM sodium ascorbate to the side of the reaction vial and then mixing the reagent with the DNA solution (Tullius et al., 1987). The final volume of the reaction mixture was 50 μL. The concentration of DNA (as moles of phosphate) in the reaction mixture was approximately 6 μM. The reaction was stopped by addition of 150 μL of a solution containing 10 mM Tris·HCl buffer (pH 8.0), 0.4% sodium dodecyl sulfate (SDS), 15 mM EDTA, 15 mM thiourea, 0.1 M NaCl, and 1 μg of carrier DNA. The mixture was extracted with 150 μL of phenol–chloroform–isoamyl alcohol and with ether before precipitation of the DNA with ethanol. The precipitated DNA was rinsed with 70% ethanol, dried, and redissolved in formamide–dye gel loading solution. DNA samples were denatured at 90 °C for 1 min before electrophoresis on a denaturing polyacrylamide sequencing gel. The percentage of polyacrylamide in the gel ranged from 6% to 8% depending on the length of the DNA fragment and the region for which high resolution was desired. Gels were dried and then exposed to preflashed X-ray film. Autoradiographs from exposures made without an intensifying screen were used to determine the locations of drug binding sites. Autoradiographs were scanned by using a Joyce Loebl Chromoscan 3 densitometer.

Footprinting with MPE·Fe(II). A solution consisting of 2.5 μM MPE (a gift from Professor Peter B. Dervan) and 2 μM ferrous ammonium sulfate was prepared, and 10 μL of this solution was added to the DNA–drug solution. The cleavage reaction was initiated by adding 5 μL of 50 mM dithiothreitol (Van Dyke et al., 1979; Hertzberg & Dervan, 1984). The reaction was allowed to proceed for 2 min before quenching as described above.

Results

Hydroxyl Radical Provides High-Resolution Footprints of

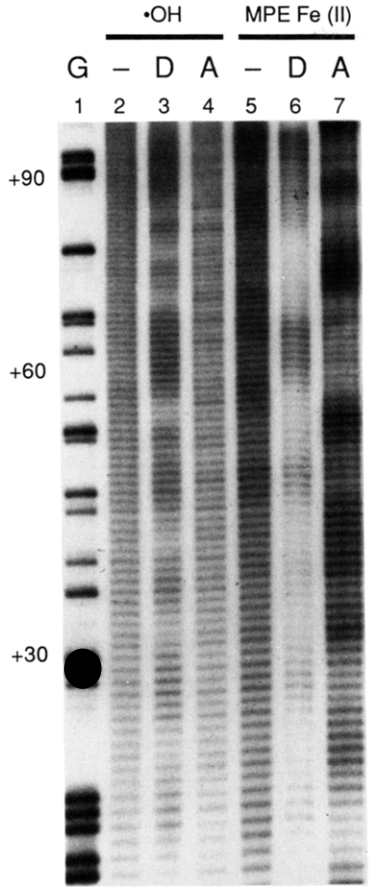

FIGURE 2: Footprinting of actinomycin and distamycin. (A) The coding strand of the Xbs 5S RNA gene, radioactively labeled on the 3′ end at the *Hin*dIII site (see Figure 1), was cleaved by itself (–) or in the presence of distamycin (D) or actinomycin (A), by the hydroxyl radical (lanes 2–4) or MPE·Fe(II) (lanes 5–7). The incubation ratios, r_i (=[drug added]/[DNA phosphate]), were 16.5 for actinomycin and 0.78 for distamycin. The products of the Maxam–Gilbert guanine-specific sequencing reaction (Maxam & Gilbert, 1980) were run in lane 1 (labeled G). (B) Diagram illustrating the sequences in the internal control region of the Xbs 5S RNA gene that are protected by distamycin and actinomycin. Solid lines represent protection by distamycin from cleavage by the hydroxyl radical, dashed lines denote protection by actinomycin from MPE·Fe(II) cleavage. Asterisks indicate positions of enhanced cleavage by the hydroxyl radical seen in the presence of bound actinomycin. The upper strand is the noncoding strand of the 5S gene.

Distamycin. We compared the abilities of two commonly used chemical footprinting reagents, the hydroxyl radical and MPE·Fe(II), to detect the binding sites of actinomycin and distamycin on DNA. Figure 2A shows an autoradiograph of a gel that is the result of such an experiment performed with the TFIIIA binding site in the somatic 5S RNA gene of *Xenopus borealis*. Lanes 2 and 5, which contain the products of cleavage of DNA without bound drug (marked –), show that the two footprinting reagents react with DNA with very little sequence preference.

Binding of distamycin was detected at the same sites by both reagents. However, the hydroxyl radical gave better definition of each distamycin binding site (compare lanes 3 and 6 in Figure 2A). Densitometer tracings of these gel lanes (not shown) demonstrate that hydroxyl radical cleavage defines a minimum binding site size for distamycin of about 4 bp. Resolution of the region between two closely bound distamycin molecules is better with the hydroxyl radical than with MPE·Fe(II). The three footprints that occur from positions +68 to +86 illustrate most clearly the ability of the hydroxyl radical to resolve closely spaced binding sites.

Actinomycin and Distamycin Give Different Types of Hydroxyl Radical Footprint. Distamycin and actinomycin bind to a number of sites along the internal control region of the 5S gene (Figure 2A,B). As has been previously noted (Van Dyke et al., 1979), distamycin binds mainly to A/T-rich regions, while actinomycin occupies G/C-rich sites. The MPE·Fe(II) footprints of both drugs are similar (Figure 2A, lanes 6 and 7), except for the positions and lengths of the protected regions. The hydroxyl radical, however, gave strikingly different cleavage patterns in the presence of the two drugs. While obvious sites of protection, like conventional footprints, are seen for distamycin (lane 3), actinomycin appears to be binding to the DNA in such a way that it does not protect the DNA from hydroxyl radical cleavage (lane 4) (Fox, 1988). Instead, the cleavage pattern in the presence of actinomycin is the same as for naked DNA, except for several isolated nucleotides that are cleaved to a greater extent, leading to the spiky appearance in the autoradiograph (lane 4). Comparison of the locations of the spikes to the locations of actinomycin binding sites determined by MPE·Fe(II) footprinting (Figure 2B) shows that the spikes appear in the middle and at the edges of actinomycin binding sites. We presume that actinomycin was bound to the DNA under the conditions of the hydroxyl radical cleavage reaction, because the same actinomycin/DNA sample gave footprints with MPE·Fe(II).

A Closer Look at the Low- and High-Affinity Distamycin Binding Sites in the 5S Gene. Previous experiments indicated that distamycin recognizes A/T-rich regions, which have a minor groove shape and hydration pattern that closely matches the van der Waals contour of the drug molecule (Coll et al., 1987). Our data show that the minimum length of A/T sequence for distamycin binding is 2 bp, as illustrated by the site at positions 54–55 (lower strand) in the 5S gene (Figure 2B). As detected by the hydroxyl radical, the distamycin protection pattern is 3–4 bases long, and the minima in protection are offset from one strand to the other by 2–3 bases, so that each binding site appears to cover around 5 bp.

Inspection of the protected sequences in Figure 2B reveals that many sites of variable A/T-rich character are bound by distamycin. Since these binding sites are occupied at rather high distamycin concentration, we refer to these as low-affinity sites. We studied the concentration-dependent binding of distamycin to much of the *Xenopus* 5S RNA gene using hydroxyl radical footprinting to monitor the number, location, and nature of the footprints as the concentration of the drug was varied. The advantage of the hydroxyl radical for making footprints of drugs is readily apparent when a range of drug concentrations is studied. Figures 3 and 4 show that both the hydroxyl radical and MPE·Fe(II) have approximately the same degree of sensitivity to low levels of bound drug. However, the hydroxyl radical clearly yields a higher resolution footprint, allowing the identification of individual closely spaced drug binding sites.

The high resolution of hydroxyl radical footprinting allows an interesting observation to be made concerning the distamycin binding that was not possible with MPE·Fe(II) footprinting. The locations of drug binding sites along the 5S gene change as the number of bound distamycin molecules increases. Inspection of the densitometer scans in Figure 4A shows that

Table I: Comparison of Distamycin Binding Sites on the Noncoding Strand of the *Xenopus borealis* 5S RNA Gene with Sites Protected from DNase I Cleavage by a Nucleosome Bound to the 5S Gene

distamycin[a]	−16	−2	+5	+15	+25	+35	+43	+57		+73	+79	+87
5S nucleosome[b]	−15	−8	+4	+12	+25	+34	+45	+55	+65	+75		

[a] This work. [b] Data from Rhodes (1985).

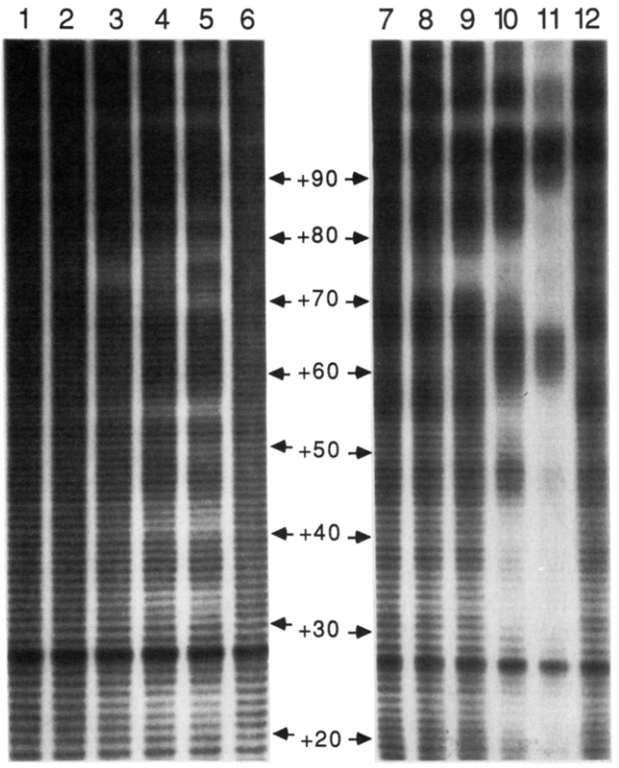

FIGURE 3: Autoradiograph showing the dependence on drug concentration of distamycin binding to the coding strand of the Xbs 5S RNA gene. For this experiment, the DNA molecule was radioactively labeled on the 3′ end at the *Hin*dIII site (see Figure 1). The incubation ratios, r_i, were 0.010 (lanes 1 and 7), 0.025 (lanes 2 and 8), 0.10 (lanes 3 and 9), 0.25 (lanes 4 and 10), 1.0 (lanes 5 and 11), and 0 (lanes 6 and 12). Lanes 1–6, footprinting with the hydroxyl radical. Lanes 7–12, footprinting with MPE·Fe(II).

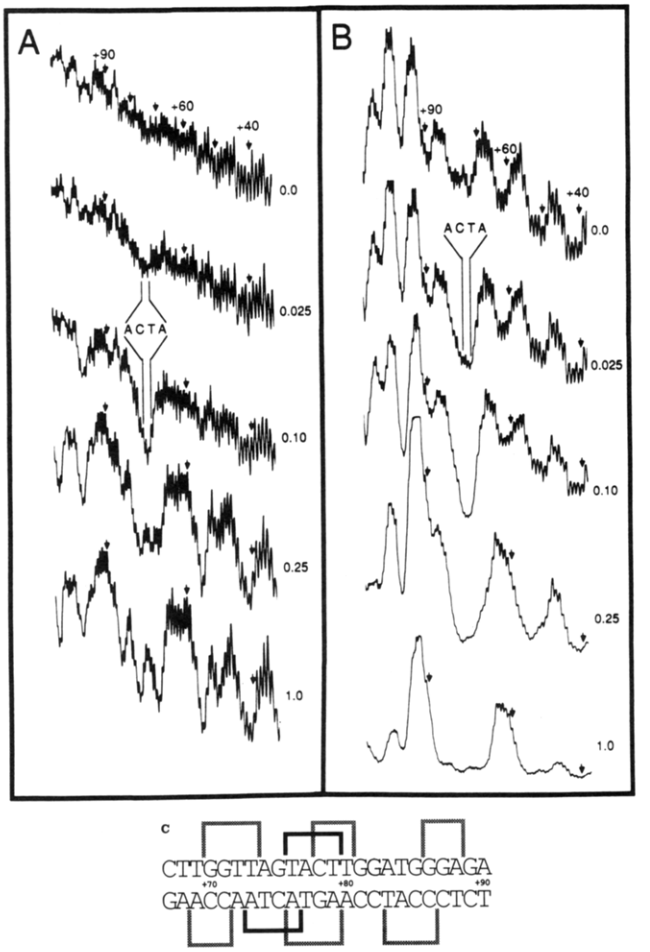

FIGURE 4: Comparison of distamycin footprints on the coding strand of the Xbs 5S RNA gene made by the hydroxyl radical and by MPE·Fe(II). Lanes in the autoradiograph depicted in Figure 3 were scanned by a densitometer. The molar ratio of distamycin added to DNA phosphate (r_i) is indicated to the right of each scan. Nucleotides are labeled in the top scan according to the numbering of the 5S gene. Vertical arrows are placed for convenience at positions +40, +60, and +90 in each scan. The high-affinity distamycin binding site that occurs at the ACTA sequence at position +74, mentioned in the text, is marked. (A) Scans of hydroxyl radical footprints. (B) Scans of MPE·Fe(II) footprints. (C) Changes in distamycin binding pattern with increasing concentration of drug, as detected by hydroxyl radical footprinting. The top strand is the noncoding strand. The high-affinity site is indicated by dark brackets, and the low-affinity sites are indicated by gray brackets. A single site that appears at positions +73 to +76 (coding strand) at low distamycin concentration is gradually replaced by three lower affinity sites on either side.

the single distamycin binding site observed at position +74 at low drug concentration is gradually replaced by an out-of-register set of three sites as the concentration of the drug increases (Figure 4C). The highest affinity site, therefore, is not occupied at high drug concentrations.

Periodic Arrangement of Low-Affinity Distamycin Sites on Three 5S RNA Genes. A remarkable feature of the low-affinity distamycin binding sites on the Xbs 5S RNA gene is the periodic arrangement of these sites on both strands over part of the gene. Hydroxyl radical footprinting shows that a distamycin molecule binds about every 10 bp from around +1 to around +60 (Figure 5). We noticed that these sites were well correlated with the structure of a nucleosome that has been reconstituted on the Xbs 5S gene in the region from +78 to approximately −85 relative to the start of transcription (Rhodes, 1985; Losa & Brown, 1987). The DNA sequences that are protected by the nucleosome core particle (the sequences with their minor grooves facing inward) correspond well with those that are bound by distamycin from +1 to +60. A summary of these data is presented in Table I.

There is evidence in the literature that the somatic and oocyte 5S genes of *Xenopus laevis* (Xls and Xlo) may differ from the somatic 5S gene of *Xenopus borealis* (Xbs) in the position at which a nucleosome core forms on the gene (Gottesfeld, 1987). There are, however, only a few differences in base sequence among the three genes. We examined the Xls and Xlo 5S genes for distamycin binding to determine whether these genes also bind distamycin in a periodic way. The results of these experiments are shown in the three densitometer scans in Figure 6. Figure 7 shows an alignment of the DNA sequences of the three 5S genes.

Most of the distamycin binding sites remain the same as for the Xbs gene despite as many as 15 sequence changes in the region −20 to +60. One distamycin binding site, though, completely disappears in the Xls and Xlo genes. Apparently because of the change of a T (at +12) to a C in the sequence ATAC, giving ACAC, distamycin binding is lost at site +15 for both the Xls and Xlo genes. In the region from −2 to +29,

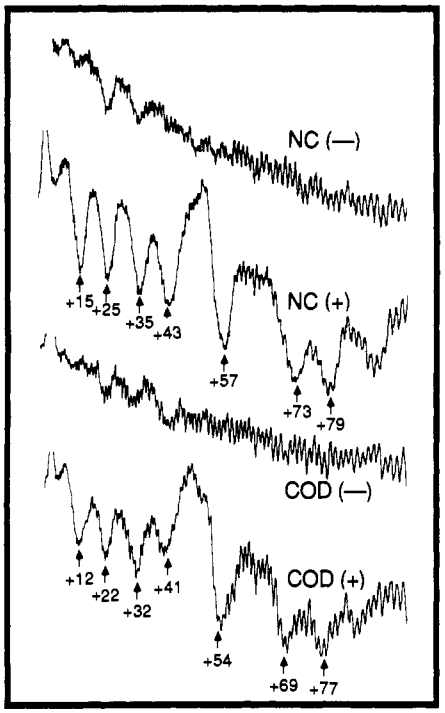

FIGURE 5: Periodic pattern of hydroxyl radical footprints of distamycin bound to the Xbs 5S RNA gene. The *Bam*HI–*Hin*dIII restriction fragment, labeled 5′ or 3′ at the *Bam*HI end (see Figure 1), was used to observe distamycin binding. The incubation ratio, r_i, was 0.78. NC, noncoding strand; COD, coding strand; (−), no distamycin present; (+), distamycin bound to 5S DNA.

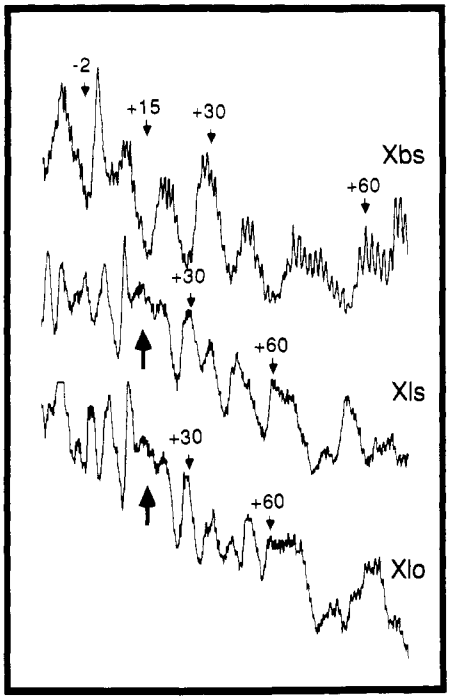

FIGURE 6: Densitometer scans illustrating the differences in the binding of distamycin to the Xbs, Xls, and Xlo 5S RNA genes as detected by hydroxyl radical footprinting. The products of cleavage of the noncoding strands of the Xbs (top), Xls (middle), and Xlo (bottom) 5S genes in the presence of distamycin (r_i = 0.78) were electrophoresed for different times so that the cleavage patterns near the 5′ ends of the three genes could be compared. Fragments were radioactively labeled on the 3′ end of the DNA at the *Bam*HI site (Xbs), the *Sal*I site (Xls), or the *Hin*dIII site (Xlo) (see Figure 1). Nucleotides were identified by comparison with a marker lane containing products of guanine-specific cleavage. Heavy arrows point to the place at around +15 in the Xls and Xlo genes where distamycin binding is most obviously different from that found for the Xbs gene. Other sites differ as well, though not to as great an extent.

there is only 1 bp difference among the genes, and one large change in distamycin binding results. The extensive sequence changes in the region −13 to −3 result in little observable change in drug binding.

Discussion

Features of Antibiotic Binding Detected by the Hydroxyl Radical. Distamycin and actinomycin have different modes of binding to the minor groove of DNA: one binds within the groove, while the other intercalates between base pairs. The hydroxyl radical protection patterns appear to reflect this difference. Actinomycin hardly protects the DNA from cleavage by the hydroxyl radical. Instead, actinomycin induces hyperreactivity of certain deoxyriboses along the phosphodiester backbone. Besides footprints, DNase I cleavage patterns of actinomycin–DNA complexes also exhibit hypersensitive nucleotides next to the binding site (Lane et al., 1983). Hypersensitivity to DNase I appears to depend on the sequence flanking the actinomycin binding site (Huang et al., 1988). Structural analysis of other intercalator–DNA complexes showed that the sugar 3′ to the intercalation site is often found in the C3′-endo conformation, rather than the C2′-endo conformation normally found in B-DNA (Neidle & Abraham, 1984). The rate of cleavage of a particular nucleotide by the hydroxyl radical might conceivably be sensitive to the conformation of the deoxyribose. The spikes in the hydroxyl radical cleavage pattern may therefore be due to a sugar adjacent to the intercalation site having a conformation that is different from the usual.

The minimum sequence required for low-affinity distamycin binding appears to be AT or AA. The observed concentration-dependent redistribution of distamycin binding sites near position +74 (Figures 3 and 4A, C) is likely due to the presence of several overlapping binding sites. At low drug concentration, the highest affinity site is occupied, but as the distamycin concentration is raised, more binding energy is available from occupation of three weaker binding sites than from the one strong site. Alternatively, a cooperative interaction of the drug with DNA (Hogan et al., 1979) might also explain this observation. At r_b = [bound drug]/[DNA base pairs] = 0.03, distamycin was found to bind to calf thymus DNA approximately 15 times more strongly than at lower r_b, apparently because of a drug-induced conformational change in the DNA (Hogan et al., 1979). If the ratios of bound drug to DNA in the present experiments lie in that range, and if the 5S gene behaves like calf thymus DNA in its interaction with distamycin, then sites previously inaccessible to distamycin would be transformed into binding sites as the result of the drug molecules bound at neighboring sites. The molar ratio of drug added to DNA phosphates, r_i, in some of our experiments was high (r_i = 0.78, for example). However, not all of the added distamycin is bound, and depending on the intrinsic binding constant, r_b would be at least 2 times, and perhaps as much as 300 times, lower than r_i. [These calculations are based on the intrinsic binding constants suggested by Hogan et al. (1979).] It therefore could be that in our footprint titration experiments we are witnessing the effect of bound drug on the structure of DNA. Since the shapes of the distamycin footprints in low- and high-affinity sites are comparable, the mode of binding is also likely to be similar, supporting the notion that the conformation of the DNA changes with increasing amounts of bound distamycin (Coll et al., 1989).

Distamycin as a Probe of the Structure of the 5S RNA Genes of Xenopus. Previous work indicated that distamycin

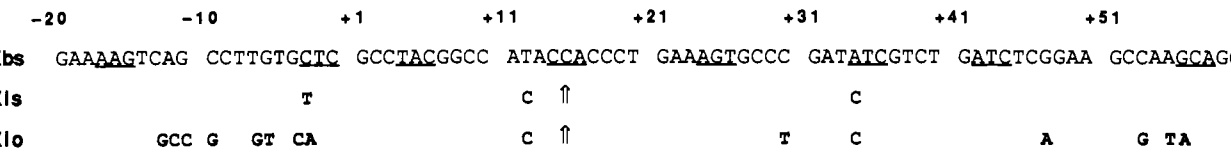

FIGURE 7: Alignment of the sequences of the noncoding strands of the Xbs, Xls, and Xlo 5S genes from positions −20 to +60. Boldface letters denote the nucleotides at which the Xls and Xlo sequences differ from the Xbs sequence. Underlining indicates distamycin binding sites found on the noncoding strand of the Xbs gene. Note that protection on the coding strand would be offset by roughly two bases in the 3′ direction. The upward arrow points out the place where a distamycin binding site in the Xbs gene is shown by hydroxyl radical footprinting not to exist in the Xls and Xlo genes (see Figure 6).

binding requires a definite minor groove shape, found in A/T-rich regions of B-DNA, which differs from the shallow, flat minor groove associated with A-DNA (Zimmer & Wähnert, 1986; Kopka et al., 1985a,b; Lavery et al., 1986). We used distamycin as a probe of the shape of the minor groove of the TFIIIA binding site (internal control region) in the 5S RNA gene of *Xenopus*. Nuclease cleavage experiments, X-ray crystallography, and circular dichroism spectroscopy (Rhodes & Klug, 1986; McCall et al., 1986; Fairall et al., 1989) have provided evidence that at least portions of the 5S gene are unlike B-DNA in conformation.

The DNase I digestion pattern of the internal control region shows a periodicity of 5.7 bp (Rhodes & Klug, 1986). Twice this repeat is 11.4 bp, similar to the helical repeat characteristic of A-DNA. McCall et al. (1986) crystallized an oligonucleotide with the sequence of the segment (+81 to +89) of the internal control region that has the strongest interaction with TFIIIA. The structure of this DNA molecule in the crystal has the characteristics of an A-DNA helix, although with some notable variations. The helical repeat of the oligonucleotide was calculated to be 11.5 bp/turn. The major groove is deep and wide, intermediate in shape between that of canonical A- and B-DNA. The minor groove is fairly shallow. Other helical parameters such as roll and tilt resemble those found in RNA.

Circular dichroism experiments were interpreted to indicate that the structures in solution of both the 5S gene and this particular oligonucleotide lie somewhere between B-DNA and RNA (Fairall et al., 1989). The results of NMR experiments, however, show that the deoxyriboses in the same oligonucleotide exist in the C2′-endo conformation (Aboul-ela et al., 1988), characteristic of B-DNA. The results of UV photofootprinting experiments (Becker & Wang, 1989) suggest that under normal solution conditions the sea urchin 5S gene exists in the B-DNA conformation but that particular regions undergo transitions to a more A-DNA-like conformation as the concentration of trifluoroethanol is raised. The structure in solution of the TFIIIA binding site therefore is still a matter of discussion.

Our experiments show that distamycin binds both within and outside the internal control region. There are, though, two stretches of DNA in the internal control region where distamycin does not bind (even at high concentration), located from +44 to +53 and from +57 to +68 (coding strand). An unexpected observation is that a low-affinity distamycin binding site occurs at position +85, which is in the middle of a 5S DNA sequence that crystallized as A-type DNA (McCall et al., 1986). Since distamycin binding may be an indication of a relatively narrow minor groove, and not wide as in A-DNA, the appearance of distamycin binding sites in this region suggests either that the minor groove in this region is B-DNA-like or that it adopts an intermediate structure that can be transformed into B-DNA at high drug concentrations.

A surprising observation is that the site in the region of the 5S gene that we studied for which distamycin has the highest affinity does not fit the accepted explanation for the DNA sequence preference of this drug (Kopka et al., 1985a). At the lowest concentrations at which distamycin binding is detectable, only the ACTA sequence centered at +74 (coding strand) shows protection from hydroxyl radical cleavage. Distamycin binds preferentially to this position even though a G·C base pair occurs in the center of the site. Several other sites, made up of runs of adenines, that conform well to the previously determined sequence preference of distamycin are unoccupied while the +74 site is filled. Thus, the argument that the 2-amino group of guanine hinders binding of distamycin to G·C-containing sites apparently does not always hold (Youngquist & Dervan, 1985).

Biological Implications. Satchwell et al. (1986), using Fourier analysis techniques, noted that regions 27, 36, 47, and 56 bp from the end of nucleosome core DNA have a higher probability than random-sequence DNA of being short runs of A or T. These regions correspond to positions +44, +35, +24, and +15 in the 5S RNA gene, which have been shown to be places where the minor groove of the DNA faces in toward the protein core of the positioned nucleosome that assembles on this gene (Rhodes, 1985) (Table I). The ability of such DNA sequences to assemble into specifically positioned nucleosomes is thought to be related to the well-known propensity of phased runs of A/T sequences to bend (Drew & Travers, 1985; Travers & Klug, 1987).

We find that distamycin binds to the 5S RNA gene at an array of sites that would be located on the inside of the DNA superhelix in a nucleosome. In addition, distamycin binding sites often correspond to regions of the 5S gene that are protected from hydroxyl radical cleavage when this DNA molecule is bound to a precipitate of calcium phosphate, and in some cases with places in the naked 5S gene at which low rates of cleavage by the hydroxyl radical occur (Churchill, 1987; Hayes, Tullius, and Wolffe, submitted for publication). Although we have not yet fully explored these other observations, when considered together with the data presented here a clear indication emerges that DNA structure plays an important role in the positioning of nucleosomes (Drew & Travers, 1985).

Our observations suggest that distamycin could be a useful probe to identify the array of sequence signals that control nucleosome positioning, which might not be apparent from simple inspection of a sequence. Drew and Travers (1985) took advantage of the sequence preferences of distamycin to map the occurrence of A/T-rich regions in bulk nucleosomal DNA by a method they called "statistical sequencing". The average positions of distamycin binding that they determined using this collection of nucleosomal DNA molecules generally correspond well with the places where we find distamycin to be bound in the particular nucleosomal DNA molecule from the Xbs 5S gene.

Although the Xls gene is closely related to the Xbs gene, the Xls gene has been reported to bind a nucleosome in a distinctly different position, starting at approximately position

+20 and extending to about +180 (Gottesfeld, 1987). We detect an interesting difference in distamycin binding between the Xls and Xbs 5S genes. A 21 bp stretch of DNA in the Xls gene that is refractory to distamycin binding occurs where a single base pair (+12) differs between the Xls (5′-ACAC-3′) and Xbs (5′-ATAC-3′) genes. A related 5S gene from *Lytechinus variegatus* has the sequence ATAC at +11 to +14 on the noncoding strand that occurs in the Xbs gene, and a nucleosome is positioned in the same place in the two genes, despite numerous differences between the rest of the two sequences (Simpson & Stafford, 1983). The loss of this distamycin binding site in the Xls gene might indicate a sequence that is no longer compatible with the severely curved DNA found in the nucleosome (Travers & Klug, 1987). This may account for the different locations of positioned nucleosomes reported for the Xbs and Xls genes. Singlet oxygen has been found to react with the DNA of nucleosome core particles at a specific site (Hogan et al., 1987) that corresponds to position +12 in the 5S gene, evidence that perhaps the DNA at this site must be capable of adopting a peculiar conformation when in a nucleosome.

Conclusions

We have used the method of hydroxyl radical footprinting to map the positions of binding of two small molecules, actinomycin and distamycin, to 5S ribosomal RNA genes of *Xenopus*. While bound actinomycin does not give rise to a conventional footprint, high-resolution footprints of distamycin are produced by the hydroxyl radical. At low distamycin concentration, the drug occupies a site with a G·C base pair at the center, an unusual choice given previous conclusions that A/T-rich sequences are favored by the drug. At high concentrations, we find that distamycin binds in a periodic fashion within and around the *Xenopus borealis* 5S gene, with its binding sites coinciding with places where the minor groove of the DNA would face the protein core of the nucleosome that binds to this segment of DNA. A change in the distamycin binding pattern is seen in DNA from a species of *Xenopus* that is thought to have a nucleosome bound to a different site. Distamycin therefore appears to sense particular structural (or perhaps dynamic) features of DNA that may also be involved in positioning of nucleosomes.

Acknowledgments

We thank Daniela Rhodes and Andrew Travers for helpful discussions and comments on the manuscript.

Registry No. Hydroxyl radical, 3352-57-6; distamycin, 39389-47-4; actinomycin, 1402-38-6.

References

Aboul-ela, F., Varani, G., Walker, G. T., & Tinoco, I. (1988) *Nucleic Acids Res. 16*, 3559–3572.

Becker, M. M., & Wang, Z. (1989) *J. Biol. Chem. 264*, 4163–4167.

Bogenhagen, D. F., Sakonju, S., & Brown, D. D. (1980) *Cell 19*, 27–35.

Churchill, M. E. A. (1987) Dissertation, The Johns Hopkins University, Baltimore, MD.

Coll, M., Fredrick, C. A., Wang, A. H.-J., & Rich, A. (1987) *Proc. Natl. Acad. Sci. U.S.A. 84*, 8385–8389.

Coll, M., Aymami, J., van der Marel, G. A., van Boom, J. H., Rich, A., & Wang, A. H.-J. (1989) *Biochemistry 28*, 310–320.

Cons, B. M. G., & Fox, K. R. (1989a) *Biochem. Biophys. Res. Commun. 160*, 517–524.

Cons, B. M. G., & Fox, K. R. (1989b) *Nucleic Acids Res. 17*, 5447–5459.

Drew, H. R., & Travers, A. A. (1985) *J. Mol. Biol. 186*, 773–790.

Fairall, L., Martin, S., & Rhodes, D. (1989) *EMBO J. 8*, 1809–1817.

Feigon, J., Denny, W. A., Leupin, W., & Kearns, D. R. (1984) *J. Med. Chem. 27*, 450–465.

Fox, K. R. (1988) *Anti-Cancer Drug Des. 3*, 157–168.

Fox, K. R., & Waring, M. J. (1984) *Nucleic Acids Res. 12*, 9271–9285.

Gottesfeld, J. M. (1987) *Mol. Cell. Biol. 7*, 1612–1622.

Hertzberg, R. P., & Dervan, P. B. (1984) *Biochemistry 23*, 3934–3945.

Hogan, M., Dattagupta, N., & Crothers, D. M. (1979) *Nature 278*, 521–524.

Hogan, M. E., Rooney, T. F., & Austin, R. H. (1987) *Nature 328*, 554–557.

Huang, Y. Q., Rehfuss, R. P., LaPlante, S. R., Boudreau, E., Borer, P. N., & Lane, M. J. (1988) *Nucleic Acids Res. 16*, 11125–11139.

Kopka, M. L, Yoon, C., Goodsell, D., Pjura, P., & Dickerson, R. E. (1985a) *J. Mol. Biol. 183*, 553–563.

Kopka, M. L., Yoon, C., Goodsell, D., Pjura, P., & Dickerson, R. E. (1985b) *Proc. Natl. Acad. Sci. U.S.A. 82*, 1376–1380.

Klevit, R. E., Wemmer, D. E., & Reid, B. R. (1986) *Biochemistry 25*, 3296–3303.

Kuwabara, M., Yoon, C., Goyne, T., Thederahn, T., & Sigman, D. S. (1986) *Biochemistry 25*, 7401–7408.

Lane, M. J., Dabrowiak, J. C., & Vournakis, J. N. (1983) *Proc. Natl. Acad. Sci. U.S.A. 80*, 3260–3264.

Lavery, R., Kakrzewska, K., & Pullman, B. (1986) *J. Biomol. Stereodyn. 3*, 1155–1170.

Losa, R., & Brown, D. D. (1987) *Cell 50*, 801–808.

Maxam, A. M., & Gilbert, W. (1980) *Methods Enzymol. 57*, 499–559.

McCall, M., Brown, T., Hunter, W. N., & Kennard, O. (1986) *Nature 322*, 661–664.

Miller, J. R., Cartwright, E. M., Brownlee, G. G., Fedoroff, N. V., & Brown, D. D. (1978) *Cell 13*, 717–725.

Neidle, S., & Abraham, Z. (1984) *CRC Crit. Rev. Biochem. 17*, 73–121.

Patel, D. J. (1982) *Proc. Natl. Acad. Sci. U.S.A. 79*, 6424–6428.

Patel, D. J., Pardi, A., & Itakura, K. (1982) *Science 216*, 581–590.

Pelton, J. G., & Wemmer, D. E. (1988) *Biochemistry 27*, 8088–8096.

Pelton, J. G., & Wemmer, D. E. (1989) *Proc. Natl. Acad. Sci. U.S.A. 86*, 5723–5727.

Portugal, J., & Waring, M. J. (1987) *FEBS Lett. 225*, 195–200.

Rhodes, D. (1985) *EMBO J. 4*, 3473–3482.

Rhodes, D., & Klug, A. (1986) *Cell 46*, 123–132.

Satchwell, S. C., Drew, H. R., & Travers, A. A. (1986) *J. Mol. Biol. 191*, 659–675.

Simpson, R. T., & Stafford, D. W. (1983) *Proc. Natl. Acad. Sci. U.S.A. 80*, 51–55.

Smith, D. R., Jackson, I. J., & Brown, D. D. (1984) *Cell 37*, 645–652.

Travers, A. A., & Klug, A. (1987) *Philos. Trans. R. Soc. London 317*, 537–561.

Tullius, T. D. (1987) *Trends Biochem. Sci. 12*, 297-300.
Tullius, T. D., Dombroski, B. A., Churchill, M. E. A., & Kam, L. (1987) *Methods Enzymol. 155*, 537-558.
Van Dyke, M. W., Hertzberg, R. P., & Dervan, P. B. (1979) *Proc. Natl. Acad. Sci. U.S.A. 79*, 5470-5474.
Ward, B., Rehfuss, R., Goodisman, J., & Dabrowiak, J. C. (1988) *Nucleic Acids Res. 16*, 1359-1369.
Wolffe, A. P., & Brown, D. D. (1987) *Cell 51*, 733-740.
Youngquist, R. S., & Dervan, P. B. (1985) *Proc. Natl. Acad. Sci. U.S.A. 82*, 2565-2569.
Zimmer, C. (1975) *Prog. Nucleic Acid Res. Mol. Biol. 1*, 399-411.
Zimmer, C., & Wähnert, U. (1986) *Prog. Biophys. Mol. Biol. 47*, 31-112.
Zimmer, C., Kakiuchi, N., & Guschlbauer, W. (1984) *Nucleic Acids Res. 10*, 1721-1732.

Sequence Preferences of Covalent DNA Binding by *anti*-(+)- and *anti*-(−)-Benzo[*a*]pyrene Diol Epoxides†

Randolph L. Rill* and Glenn A. Marsch
Department of Chemistry and Institute of Molecular Biophysics, The Florida State University, Tallahassee, Florida 32306
Received November 27, 1989; Revised Manuscript Received January 17, 1990

ABSTRACT: The sequence preferences of formation of piperidine-labile adducts of guanine by individual (+)- and (−)-isomers of *trans*-7,8-dihydroxy-*anti*-9,10-epoxy-7,8,9,10-tetrahydrobenzo[*a*]pyrene [anti-(+)- and anti-(−)-BPDE] were examined by techniques analogous to chemical DNA sequencing. Data were obtained on over 1200 bases with *anti*-(−)-BPDE and 1000 bases with *anti*-(+)-BPDE. Guanines on average yielded more labile adducts than other bases, and the reactivities of guanines with both *anti*-(+)- and *anti*-(−)-BPDE isomers were found to be distinctly nonrandom with respect to DNA sequence. The most and least reactive guanines, defined in terms of the upper and lower 10 percentiles of reactivity, differed on average by a factor of 17. This range of guanine reactivities was correlated with distinct sequence preferences, which differed in part for the two isomers. The strongest determinant for preferred reaction of *anti*-(−)-BPDE to form a labile adduct at a guanine was the presence of a 3′-flanking guanine, but a thymine 5′-flanking a guanine also generally enhanced reactivity. The triplets containing central guanines most preferred by *anti*-(−)-BPDE were AGG, CGG, and TG(G>T>C,A). *anti*-(+)-BPDE also formed labile adducts preferentially at AGG and CGG triplets, but not at TGN triplets. Significant effects of next-nearest-neighbor bases on guanine reactivities were also noted.

Benzo[*a*]pyrene (B[a]P)[1] is a prototypical carcinogen of the polycyclic aromatic hydrocarbon class and was one of the first verified examples of a chemical carcinogen [reviewed by Phillips (1983) and Gräslund and Jernström (1989)]. B[a]P is not direct acting but is metabolically activated in vivo to the ultimate carcinogenic forms, the benzo[*a*]pyrene diol epoxides (BPDE's). Of the many possible stereoisomers of BPDE, the (7*R*,8*S*)-dihydroxy-(9*S*,10*R*)-epoxy-7,8,9,10-tetrahydro-B[a]P isomer [anti-(+)-BPDE] is both the most abundant product formed in vivo in most tissues [Yang & Gelboin, 1976; Thakker et al., 1977; Yang et al. 1977; Deutsch et al., 1978; Harvey, 1981; Conney, 1982; isomer named according to Gräslund and Jernström (1989)] and the most potent carcinogen in mammalian systems (Thakker et al., 1976; Buening et al., 1978; Slaga et al., 1979; Harvey, 1981; Conney, 1982).

Both the *anti*-(+)- and *anti*-(−)-BPDE isomers bind covalently to DNA via predominantly trans addition of base nucleophiles at the 10-position of the highly reactive BPDE epoxide ring (Weinstein et al., 1976; Jeffrey et al., 1976; Osborne et al., 1976, 1978). Addition occurs mainly at the guanine N^2-amino group and is stereoselective: *anti*-(+)-BPDE reacts much more readily at this position than the anti-(−)-isomer (Weinstein et al., 1976; Jeffrey et al., 1976, 1977; King et al., 1976; Meehan & Straub, 1977; Osborne et al., 1981; Brookes & Osborne, 1982). BPDE adducts at guanine N^2 are stable to alkali. Additional, *alkali-labile* adducts are formed on other base sites, however, particularly on the guanine N7 ring nitrogen (Osborne et al., 1978; 1981; King et al., 1979; Sage & Haseltine, 1984). Sage and Haseltine (1984) recently showed that alkali-labile adducts are formed in larger yields than previously suggested, accounting for up to 40% of the total adducts formed by racemic (±)-*anti*-BPDE. About 60% of the alkali-labile products occurred on G's, and formation of alkali-labile adducts was found to be nonrandom with respect to base sequence.

Linear dichroism and fluorescence studies have been able to differentiate between two distinct conformations of BPDE adducts termed types I and II [reviewed by Gräslund and Jernström (1989)]. The pyrene moieties of type I adducts are more perpendicular than parallel to the DNA helix axis and are protected from solvent. In type II adducts the pyrenes are more exposed and more parallel than perpendicular to the helix axis. *anti*-(+)-BPDE–DNA adducts consist almost entirely of the type II conformers, but *anti*-(−)-BPDE–DNA adducts are a nearly equal mixture of type I and type II conformers.

† Supported by Grant ER60588 from the U.S. Department of Energy.
* Corresponding author.

[1] Abbreviations: *anti*-(+)-BPDE, 7(*R*),8(*S*)-dihydroxy-9(*S*),10(*R*)-epoxy-7,8,9,10-tetrahydrobenzo[*a*]pyrene; *anti*-(−)-BPDE, the enantiomer of *anti*-(+)-BPDE; B[a]P, benzo[*a*]pyrene; BPDE, *trans*-7,8-dihydroxy-9,10-epoxy-7,8,9,10-tetrahydrobenzo[*a*]pyrene; DMSO, dimethyl sulfoxide; MOPS, 3-(*N*-morpholino)propanesulfonic acid.

0006-2960/90/0429-6050$02.50/0